Aus dem Institut/der Klinik für Neurochirurgie
der Medizinischen Fakultät Charité – Universitätsmedizin Berlin

DISSERTATION

Antitumor effect of PEG-ZnPP in Rat Glioma Cells, F98 and C6, and in Rat Brainstem Tumor Models

zur Erlangung des akademischen Grades
Doctor medicinae (Dr. med.)

vorgelegt der Medizinischen Fakultät
Charité – Universitätsmedizin Berlin

von

Young Sill Kang
aus Daegu, Südkorea

Datum der Promotion: 13. December 2019

Table of Contents

Abbreviations

AMT	Adsorptive Mediated Transcytosis
BBB	Blood–Brain Barrier
CdK	Cyclin-dependent Kinase
CED	Convection Enhanced Delivery
CKI	Cyclin-dependent Kinase Inhibitor 1
CNS	Central Nervous System
D	Daltons
DIPG	Diffuse Intrinsic Pontine Glioma
DMEM	Dulbecco's Modified Eagle Medium
EC	Endothelial Cells
FBS	Fetal Bovin Serum
HO-1	Heme Oxgenase 1
I.V.	Intra Venous
PBS	Phosphate-Buffered Saline
PEG-ZnPP	Pegylated Zinc Protoporphyrin
PI	Phosphatidyl Inositol
Rb	Retinoblastoma protein
RMT	Receptor-Mediated Transcytosis
ROS	Reactive Oxygen Species
SiRNA	small interfering Ribonuclease
V-FITC	V-Fluorescein Isothiocyanate
VEGF	Vascular Endothelial Growth Factor
ZnPP	Zinc Protoporphyrin

“Something the Lord made”

1. Abstract

1.1. English Version

Objective: Brainstem tumors account for about 10-20% of all primary paediatric tumors in the central nervous system. Approximately 75% of all brainstem tumors in children are diffuse pontine gliomas (DIPG) and the median overall survival is less than a year. Due to its infiltrative character and anatomical location, surgical resection is not considered as therapeutic option. It was described that expression of HO-1 is associated with growth activity of cancer cells, which suggests that a specific inhibitor of HO-1, ZnPP, may work as a potent antitumor therapeutic agent. To evaluate the antitumor efficacy of PEG-ZnPP, a water soluble derivate of ZnPP, we performed studies *in vitro* and *in vivo* brainstem glioma models.

Methods: To evaluate the antitumor efficacy of PEG-ZnPP *in vitro*, proliferation assay on glioma cell lines C6 and F98 was performed. Based on the results of our proliferation assay, apoptotic activity using conjugate of annexin V was evaluated and cell cycle analysis was assessed. After *in vitro* study, we performed systemic therapy with PEG-ZnPP in rat brainstem tumor models with F98 and C6. Neurological status and survival rate was monitored.

Results: This project demonstrated that PEG-ZnPP significantly inhibits rat glioma cell proliferation and induces a significant level of apoptosis in C6 and F98 glioma cell lines, suggesting that PEG-ZnPP may represent a potential anticancer agent for brain tumors. *In vivo* study on rat brainstem glioma models, however, showed no differences of survival between the control group and animals receiving intravenous PEG-ZnPP therapy.

Conclusion: In contrast to *in vitro* studies systemic administration of PEG-ZnPP did not improve the survival on the rat brainstem glioma model suggesting that different approaches and additional animal research are required to overcome the BBB and to further investigate the potential anticancer abilities of PEG-ZnPP.

1.2. Deutsche Version

Einleitung: Tumore des Hirnstamms machen ca. 10-20% aller primären Tumoren des zentralen Nervensystems im Kindesalter aus. Zirka 75% aller Tumore im Hirnstamm sind die diffus intrinsischen Ponsgliome (DIPG) und deren mediane Lebenserwartung beträgt weniger als ein Jahr. Aufgrund des infiltrativen Charakters und deren Lokalisation kommt die Resektion als therapeutische Option nicht in Frage. Es ist bekannt, dass erhöhte Expression der HO-1 mit einem raschen Wachstum von Tumorzellen assoziiert ist, sodass eine spezifische Inhibition der HO-1 mittels PEG-ZnPP, eine wasserlösliche Form von ZnPP, als eine anti-tumorale Therapie möglich erscheinen lässt. In dieser Studie wurde antitumorale Wirkung von PEG-ZnPP innerhalb von in vitro Analyse und in vivo im Hirnstammgliom Modell bei der Ratte durchgeführt.

Methoden: In der vitro Untersuchung erfolgte zur Evaluation der antitumoren Effektivität eine Proliferationsanalyse in den F98 und C6 Gliomzelllinien. Anschließend erfolgte in einer vivo Studie die Implantation von F98 und C6 Gliomzellen in den Hirnstamm der Ratte gefolgt von einer systemischen Gabe von PEG-ZnPP. Der neurologische Status und das Körpergewicht der Ratte wurden im Verlauf dokumentiert und die Überlebensrate der Tiere bestimmt.

Ergebnisse: Diese Studie konnte in den in-vitro Untersuchungen die signifikante Hemmung der Gliomzell-Proliferation durch PEG-ZnPP zeigen. Demgegenüber zeigten die in-vivo Untersuchungen keine Unterschiede der Überlebensrate der PEG-ZnPP behandelten Tiere im Vergleich zu den Kontrolltieren.

Schlussfolgerung: Trotz der antitumoralen Wirkung von PEG-ZnPP in vitro zeigte die systemische Applikation im Hirnstammgliom Modell keine überlebensverlängernde Wirkung der Ratte. Am ehesten scheint die Blut-Hirn-Schranke eine relevante Barriere für PEG ZnPP zu sein welches diese Diskrepanz erklären könnte. Als Herausforderung bleibt neue Versuchsverfahren zur Überwindung der Blut-Hirn-Schranke zu finden, um die antitumore Wirksamkeit von PEG-ZnPP in-vivo testen zu können.

2. Introduction

2.1. Brainstem Glioma

Brainstem tumors refer to heterogeneous tumor lesions in the midbrain, the pons or the medulla oblongata. These tumors are uncommon in adults, but in children represent 15-20% of all primary paediatric tumors in the CNS [1, 2]. Brainstem glioma can be subdivided into focal and diffuse subtypes. Further classification of the brainstem glioma is various. Typically brainstem tumors can be classified according to MR imaging and divided according to their location in the midbrain, pons or medulla [3]. Currently based on anatomical characters on the MR imaging, it can be classified into the following subgroups: tectal tumors, diffuse intrinsic pontine glioma (DIPG), focal tumors, dorsal exophytic tumors and cervicomedullary tumors [4]. It can be also classified according to imaging and predominant pathologic characteristics: diffuse intrinsic, focal midbrain, dorsal exophytic and cervicomedullary tumor type [5].

The most common tumor type among brainstem tumors is the DIPG, which accounts for 75-80% of brainstem tumors in children [6, 7]. Clinical symptoms of DIPGs and non-DIPGs include headache, vomiting, nausea, double vision, ataxia and cranial neuropathies. In cases of DIPGs, delay between first signs and the diagnosis is shorter than in cases of non-DIPG cases: less than 3 months [8]. Classic morphology of DIPG on MRI include a mass in the middle of the pons, encompassing more than 50% of the pons, and causing enlargement of the pons [8]. Some authors defined DIPG as virtually all gliomas in the diffuse masses, which occur as expansive mass lesion within the ventral pons [5]. In the majority cases with DIPG, little or no enhancement of the mass after applying of gadolinium is characteristic [8]. It is known that between 20 and 30 diffuse pontine gliomas occur in the UK annually [9] and between 100 and 150 a year in the USA [10]. DIPG is highly aggressive and prognosis is very poor. Median survival in children with diffuse brainstem glioma is less than a year [2].

2.2. Current Therapeutic Strategies

Other than DIPGs, non DIPGs including tectal, focal, dorsal exophytic and cervicomedullary tumors are typically low grade, and based upon anatomical location, size, focality of the mass and tumor growth pattern, attempts at surgical resection or biopsy can be performed [4]. In addition to surgical treatment, radiation and chemotherapy are available depending on neuropathological diagnosis.

However, due to the infiltrative character and anatomical location of the DIPGs, it has been regarded that surgical treatment is generally not possible, and due to potential complications, biopsies have been rarely performed in the past. The presumptive diagnosis of DIPG can be performed based on MR imaging characteristics, which may, however, limit potential development of the possible therapy as no tumor characteristics can be further investigated, and even a small number of cases have been reported, which were thereby misdiagnosed [8].

Since no homogenous therapy guideline for the DIPGs is available, several therapy methods including chemotherapy, adjuvant chemotherapy, and chemo-radiotherapy have been suggested, however, none of these published trials have proved significant benefit of survival yet.

Survival duration varies between trials of chemotherapy administration prior to radiotherapy, chemotherapy before and after radiotherapy, concomitant chemotherapy and radiotherapy and chemotherapy immediately following radiotherapy [1]. Neurological improvement and reduction of glucocorticoid medication could be achieved through conventional radiotherapy, but a significant association between radiotherapy and extension of overall survival has not been shown [1].

Currently, the mainstay of the treatment of DIPGs remains focal radiation therapy to the pons with 3D conformal photon-based radiotherapy to a range of 54-59.4 Gy [8]. This can be given in 30-33 fractions of 1.8 Gy daily [8]. However, the optimal fractionation has not been defined.

Multiple trials investigating benefit of combination with radiotherapy for brainstem tumor have shown disappointing results [1, 11]. Given the unsatisfactory results from current chemotherapeutic agents, better promising chemotherapeutic agents need to be explored.

2.3. Animal Model

In order to develop novel therapeutic agents, reliable experimental animal models for brainstem tumors are essential. For this purpose, an accessible and reproducible brainstem tumor model was developed by Jallo *et al.* and Thomale *et al* [12, 13]. This model shows a reproducible course of onset of neurological deficit and predictable tumor histology and allows monitoring and functional testing of rats with brainstem tumor [12]. Jallo *et al.* implanted F98 and 9L cell lines, which showed a predictable pattern of tumor infiltration, and in 80-90% of animals tumor production was confirmed [14]. This developed model is amenable to monitoring and functional testing and also demonstrated the infiltrative nature of human brainstem tumors [12].

2.4. PEG-ZnPP

2.4.1. Heme Oxygenase

HO is a microsomal enzyme and catalyses the first rate limiting step in the degradation of heme cleaving the heme to produce biliverdin, accompanied by production of carbon monoxide [15]. Iron ions and biliverdin derivated from this process play an important role in recycling of iron [16, 17]. HO cleaves the meso-carbon bridge of heme, yielding equimolar quantities of carbon monoxide (CO) [18]. Free iron induces the expression of the iron-sequestering ferritin and activates Fe-ATPase, an iron transporter, which decreases intracellular Fe_2 content [19]. Biliverdin is converted to bilirubin by biliverdin reductase [20]. Bilirubin is known as a potent antioxidant [21].

There are three identified HO isoforms catalysing heme degradation. HO-1, the oxidative stress-inducible protein, also known as HSP32 [16] and the constitutive isoenzyme HO-2 were first introduced and then HO-3, which is expressed in various organs in rats, similar to HO-2, but with a much lower catalytic activity [22]. These three isoforms are products of different genes [15].

HO-1 and HO-2 show different characteristics. It is known that HO-2 is abundant in brain and testis [23]. HO-1 is synthesized mainly in microglia, in neuronal cells and known as one of several related heme oxygenase proteins that metabolize heme to CO and biliverdin, with the release of iron [24]. Among those isoforms, HO-1 can be induced in response to various cellular stresses and oxidative stimuli including heme [25], ultraviolet irradiation [26], hydrogen peroxide [26], heavy metals [26], [27], heat shock [25], hypoxia [28] and nitric oxide (NO) [19, 29, 30]. Cells protect themselves from such stressful environments by producing protective protein, termed heat-shock protein [31].

HO-1 plays a protective role working as a potent anti-inflammatory enzyme in the cellular environment. HO-1 deficiency results in sustained oxidative stress, accentuated oxidative damage in the cardiovascular system and progressive chronic inflammation in the kidney and liver [19]. There are data suggesting that overexpression of HO-1 may defend tissues and organs from immune-mediated injury, either through protection against oxidative damage or via a local immunomodulatory influence on infiltrating inflammatory cells [32, 33]. The exact mechanism has not been elucidated. The signaling action of CO with biliverdin/bilirubin and the sequestration of the iron ion contribute to this anti-inflammatory role [19].

HO-1 works not just as an anti-inflammatory enzyme, but also as a cytoprotective enzyme in tumor cells protecting them from oxidative stress, hypoxia, serum deprivation or toxic compounds [19]. The mechanism of the anti-proliferative effect of HO-1 in many cells has not been clearly elucidated. The cytoprotective role of HO-1 for tumor cells was confirmed by studies which demonstrated that pharmacologic or genetic upregulation of HO-1 improves survival of various tumors including hepatoma [29], melanoma [34], thyroid carcinoma [35], chronic myelogenous leukemia [36], gastric cancer [37] and colon cancer cell lines [38]. Biliverdin, one of the products of heme degradation, plays an important role in protecting cells from oxidative stress by scavenging free radicals, such as peroxy radicals [39], preventing protein oxidation by the potent reactive nitrogen species peroxynitrite [40] and protecting neuronal cells from oxidative stress injury [41].

HO-1 is often upregulated in quickly proliferating cells such as cancer cells [42]. High expression of HO-1 induced by pharmacologic or genetic manipulation is associated with faster tumor growth, expressed as large volume of nodules or more numerous cancer cells [19]. Upregulation of HO-1 decreases cell proliferation, and the antiproliferative effect is reversed by HO-1 inhibition [43]. Targeted knockdown of HO-1 expression lead to growth inhibition of pancreatic cancer cells [44]

HO-1 is upregulated in various tumors including lymphosarcoma [45], adenocarcinoma [46], hepatoma [29], melanoma [47], prostate cancers [42], Kaposi sarcoma [48], squamous carcinoma [49], and pancreatic cancer [44]. There are data reporting the higher level expression of HO-1 in human brain tumors compared to the brain tissue [50]. Deininger *et al.* [51] demonstrated prominent accumulation of HO-1 expression in glioblastoma cells. Sahoo *et al.* [52] found that tumor cells utilize HO to protect themselves from oxidative stress by producing the antioxidant bilirubin.

Interestingly, expression of HO-1 in cancer cells can be further increased in response to chemotherapy and radiation [44]. Duckers *et al.* demonstrated that the upregulation of HO-1 decreases cell proliferation and inhibiting HO-1 reverses the anti-proliferative effect [43]. This finding may support that HO-1 plays an important role for regulation of cancer cells.

2.4.2. Anti-Apoptotic Effect of HO-1

One of functions of HO-1 is associated with apoptosis, which plays a pivotal role in the pathogenesis of cancer. One of the mechanisms associated with carcinogenesis is that too little programmed cell death, termed as apoptosis, occurs in cellular cascade so that defect cells are not eliminated. Apoptosis is well associated with carcinogenesis so that it is considered as an important target of anticancer treatment strategies. Anti-apoptotic efficacy of HO-1 has been demonstrated in *in vitro* and *in vivo* studies [35-38, 53]. Another important point is that anti-apoptotic effects of HO-1 can be associated with the anti-oxidative function of HO-1, as ROS are the inducers of apoptosis [54]. CO, which is one of products of HO-1, blocks the release of the mitochondrial cytochrome 1 and inhibits expression of the p53 [55]. P53 promotes apoptosis through the caspase pathway through mitochondrial cytochrome c release [56].

2.4.3. Pro-Angiogenic Effect of HO-1

HO-1 is also known as a proangiogenic enzyme. As angiogenesis is essential for tumor proliferation, understanding the mechanism of the angiogenesis may bring a key component for understanding cancer cell biology. Cisowski *et al.* demonstrated that HO-1 deficient endothelial cells can produce less VEGF than their wild type counterparts do [57], which supports the proangiogenic action of HO-1 in tumor proliferation. *In vivo* and *in vitro* experiments in the rat model, it was demonstrated that HO-1 gene transfer increased VEGF synthesis, facilitating angiogenesis, which results in improving the blood flow in *in vivo* experiments [58].

As described above, HO-1 plays a protective role for tumor cells, however it works also as a cytoprotective agent in non-cancer cells exposed to carcinogens [19]. According to Jozkowicz *et al.* [19], it can be hypothesized that HO-1 may increase the resistance of cells to harmful stimuli and cellular stresses. Currently the role of HO-1 in carcinogenesis has not been fully elucidated.

Overall the characteristics of HO-1 including angiogenesis, cytoprotection for tumor cells, carcinogenesis and anti-apoptosis contribute to tumor cell proliferation. This suggests that therapy inhibiting HO-1 may lead to cancer cell vulnerability towards oxidative stress [52], which could be utilised as potential strategic target for anticancer therapeutic development.

2.4.4. ZnPP as a Competitive Inhibitor of HO

ZnPP is a member of metalloporphyrins, in which the heme iron is replaced by zinc, and is known as a competitive HO-1 inhibitor [59, 60]. Metalloporphyrins are compounds in which the central iron of heme is replaced by other metals including chromium, cobalt, manganese, zinc or tin [61]. The function of metalloporphyrins as competitive inhibitor to HO is due to their inefficient binding to molecular oxygen, so that HO becomes unfunctional [17, 61].

2.4.5. ZnPP Conjugated with PEG

As it is validated that ZnPP can inhibit HO-1, which plays a pivotal role in tumor growth, inhibiting HO-1 and thus providing the antioxidant bilirubin, this suggests a potential therapeutic antitumor strategy. However, due to the very low solubility of the metalloporphyrin aqueous media, its utility as a systemic therapy agent has been hampered. Sahoo *et al.* [52] developed a water soluble derivative of ZnPP by conjugating it with the water soluble polymer, PEG. Aside from having its original function of ZnPP, the inhibiting of HO, this water soluble compound behaves as a macromolecular agent due to its micelle formation [52].

2.5. Enhanced Permeability and Retention Effect

In tumors, the vasculature is distinct from normal vasculature in a way that the aggressive growth of the neoplastic cells and overexpression of proangiogenic factors induce the disorganized blood vessel network. They are more permeable than normal vessels, and the density of smooth muscle cells is poor and composed of a discontinuous endothelial cell lining with an abnormal basement membranes [62, 63]. Irregular vascular shape and vessel network formation may cause poor delivery of oxygen, and consequently micro regional hypoxia can be induced [64, 65]. This hypoxic environment can cause downstream signalling of pro-angiogenic proteins, which eventually lead angiogenesis and therefore malignant progression [66, 67]. This unique feature of tumor vasculature effects on cancer therapeutic strategy. The phenomenon termed as enhanced permeability and retention (EPR) effect [52, 68] causes the tumor specific accumulation of biocompatible macromolecules and lipids when it is administered systemically [69]. According to Masumura and Maeda *et al.* [68-71], EPR effects are mainly based on the following four features: 1. Hyper-vasculature of tumor tissues. 2. Leaky structure of tumor blood vessels. 3. Enhanced production of vascular mediators including NO and bradykinin. 4. Incomplete lymphatic drainage system. These concepts were validated by demonstrating that systemic administration of conjugated ZnPP achieved effective and selective delivery of the HO inhibitor to tumor sites [52].

Maeda *et al.* found time-dependent accumulation of PEG-ZnPP in tumor tissue and gradual decrease in circulation, which may suggest that PEG-ZnPP accumulates or is deposited in solid tumor tissues after systemic administration [72]. Sahoo *et al.* reported that the enhanced permeability and retention effect of PEG-ZnPP may contribute to tumor selective targeting [52].

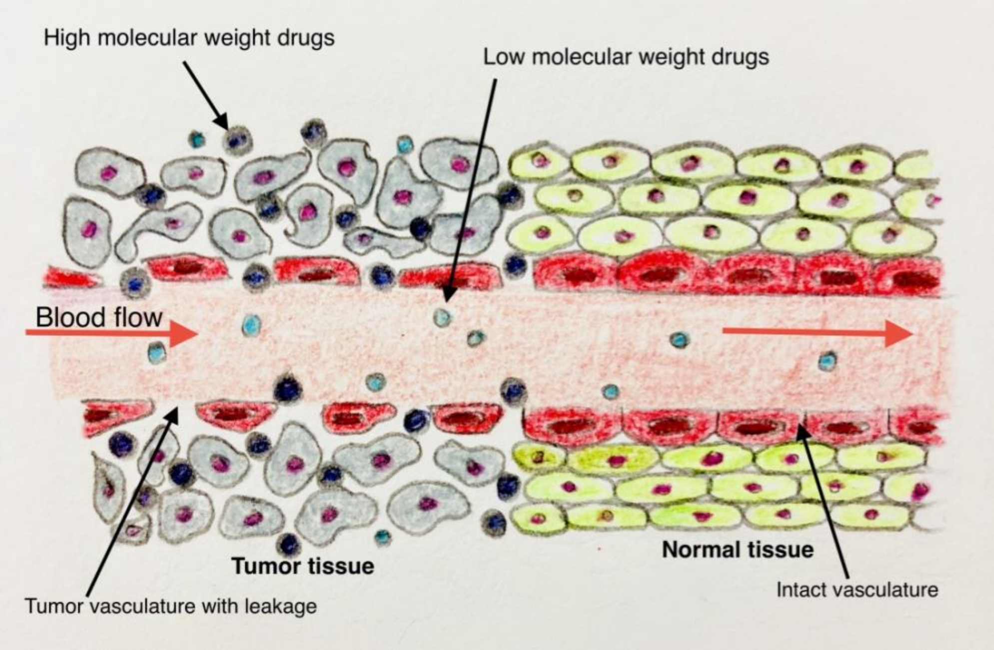

Figure 1. EPR effect [73, 74] Schematic illustration of the enhanced permeability and retention (EPR) effect of molecules with high molecular weight and low molecular weight. Due to leaky and permeable vascular structure, only few of low molecular weight stay inside the tumor tissue and the majority of them are again eliminated from the circulation rapidly. On the other hand, high molecular weight drugs including biocompatible macromolecules and lipids are distributed and accumulated in the tumor tissue. A relatively low concentration of these drugs is eliminated from the systemic circulation. Image kindly provided by YL Kang.

3. Purpose of this study

In various solid tumor models, therapy with PEG-ZnPP proved its antitumor efficacy. To our knowledge there have been no *in vitro* studies which evaluated the efficacy of PEG-ZnPP on rat glioma cell lines.

The purpose of the study was to assess the antitumor activity of PEG-ZnPP on glioma cell lines C6 and F98 proliferation in an in-vitro setup. An *in vivo* study design was to assess the effects of systemic administration of PEG-ZnPP in a rat brainstem glioma model to monitor body weight and neurological function and to evaluate the survival in response to PEG-ZnPP treatment.

4. Materials and Methods

4.1. In Vitro

4.1.1. Cell lines and culture Conditions

Two rat glioma cell lines, F98 and C6, which were purchased from the ATCC Cell Biology Collection, were used. F98 and C6 cell lines are widely used for rat brain tumor models and various studies. The F98 line was developed in BD IX rats using a single intravenous injection of N-ethyl-N-nitrosourea administered to a pregnant animal on the 20th day of gestation [75]. F98 cells show a highly invasive pattern of growth [76]. The C6 cell lines were produced by administering methyl nitrosourea to outbred Wistar rats [77, 78]. The C6 cell lines are a popular model, which is used in experimental neuro-oncology to evaluate the therapeutic anticancer efficacy [76].

These cells were routinely maintained in Dulbecco's Modified Eagle Medium (DMEM, Lonza, USA) supplemented with 10% fetal bovin serum (FBS, Gibco, Invitrogen, USA) and 1% 100 U penicillin / 0.1 mg/ml streptomycin (Invitrogen, USA) in cell culture flasks. The medium was renewed about twice a week, and the cells were subcultured while renewing the medium regularly. The cells in flasks were incubated at 37C° in 5% CO_2 humidified incubators. For washing the cells, phosphate buffered saline (PBS, pH 7.4 (1X), (-) $CaCl_2$, (-)$MgCl_2$, Gibco, USA) was used.

PEG-ZnPP was synthesized by Professor Maeda and Professor Fang (Department of Microbiology, Kumamoto University School of Medicine, 2-2-1 Honjo, Kumamoto 860-0811, Japan) [52] and kindly provided.

4.1.2. Proliferation assay

For proliferation assay, rat glioma cells, F98 and C6, were seeded at a density of 2.5×10^4 cells/well in a 6-well culture plate. These were treated with 40 µM PEG-ZnPP or phosphate buffered saline (PBS, Lonza, USA) as vehicle, grown over time in DMEM-high glucose with 10% FBS and 5% CO_2 and assessed for viable cell numbers over 6 days. The treatment with PEG-ZnPP was started 6 hours after seeding. The number of cells was monitored every other day. The final day of monitoring was day 6. This setup was repeated four times. Cells were then collected at the indicated time in 1mL of trypsin (Lonza, USA) and washed with PBS. 20 µL of cell suspension were mixed with 20 µL of Trypan Blue (Lonza, USA). Cells were counted using a Malassez slide (Invitrogen, Life Technologies, USA) and the number of cells per milliliter was determined by the following formula: n = (Cell numbers /20 squares) x 2 x 100 x 1000, in order to assess the cell proliferation over time.

4.2. In Vivo

4.2.1. Cell Preparation for the *in vivo* Study

For the *in vivo* part of the experiment, cells were carefully suspended in media and transferred to centrifuge tube for about 7 minutes. The supernatant was removed and a pellet at the bottom of the tube was suspended in a media for further cell counting. The tumor cells were counted with a hemocytometer, and were diluted with media to a concentration of 1.0×10^5 cells/3 µl. Cell preparation was done directly before the cell transplantation on the same day.

4.2.2. Animals

For the first *in vivo* experiment (Group A), a total of 17 male Sprague Dawley rats (Charles River Laboratories, Wilmington, MA, USA) weighing 250 to 350g were used. Randomly, 8 rats were assigned to control group and 9 rats to therapy group. For the second *in vivo* experiment (Group B), 15 female Fischer rats (Charles River Laboratories, Wilmington, MA, USA) weighing 130 to 160 g were used. To control group 6 rats and to therapy group 9 rats were assigned, respectively. The rats were housed in standard facilities and were given free access to Baltimore City water and rat chow. The experimental protocol was approved by the Animal Care and Use Committee of the Johns Hopkins University and the use of all study animals conformed to the National Institutes of Health Rules Guide for the Care and Use of Laboratory Animals (National Academy of Science).

4.2.3. Rat Brainstem Model - Surgery

Rats were anesthetized with an intraperitoneal injection of 3mL/kg of a stock solution containing 75 mg/mL ketamine hydrochloride (Ketathesia, Butler Animal Health Supply, USA), 7.5 mg/mL xylazine (Lloyd Laboratories, USA); and 14.25% ethyl alcohol (Fisher Scientific, USA) in 0.9% NaCl. Heads were shaved with clippers and prepared with prepodyne solution (West Penetone, USA). All surgical procedures were performed using standard sterile condition. The surgery for tumor cell implantation within the pontine brainstem was performed as described by Jallo *et al.* and Thomale *et al.* [12, 13]. In 17 Sprague Dawley rats (the first group) and 15 Fischer rats (the second group) a guide screw was positioned in a burr hole 1.4 mm right of the sagittal, and 1.0 mm anterior of the lambdoid sutures, at a depth of 7.0 mm from the dura. The head was positioned 5° from horizontal before injection of tumor cells. A 22-gauge 10-μl Hamilton needle (Hamilton Company, Reno, NV, USA) was inserted to a depth of 7 mm from the dura mater (figure 2). The first group received 3 μl of C6 glioma cells (100,000 cells) and the second group received 3 μl of F98 glioma cells (100,000 cells). To avoid cell leakage or backflow of the media, the insertion of tumor cells was performed slowly and the needle rested for 3 minutes before removal. After skin closure and recovery, the animals were returned to their cages. Each animal was subsequently evaluated for body weight changes, neurological deficits and survival time.

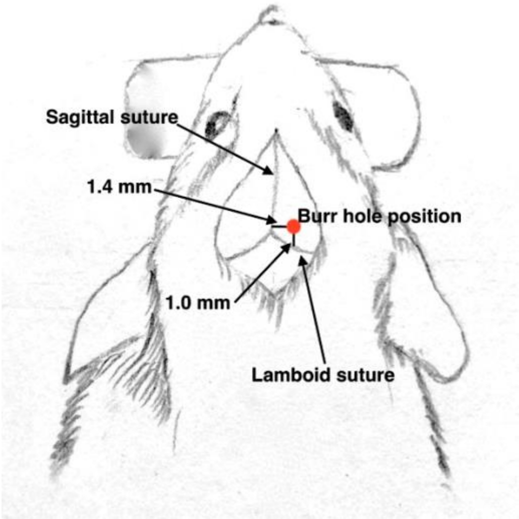

Figure 2A. Schematic illustration of surgical technique for tumor cell implantation within the pontine tegmentum. This illustration shows the position of a burr hole for tumor cell implantation. The burr hole is positioned 1.4 mm right of the sagittal and 1.0 mm anterior of the lambdoid sutures. Image kindly provided by YL Kang.

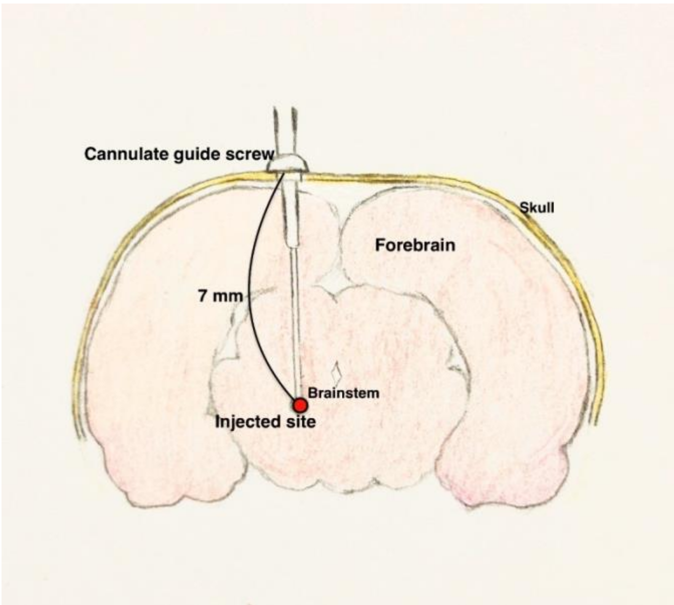

Figure 2B. This illustration shows axial section of the tumor cell implantation. After the cannulated guide screw is implanted on the calvarium, the Hamilton needle is inserted through the cannulated guide screw at the intended target, the pontine tegmentum (approximately 7 mm from dura level) [12]. Image kindly provided by YL Kang.

4.2.4. Systemic administration

In the first *in vivo* trial on Sprague Dawley rats (Group A), intravenous treatment with PEG-ZnPP was begun on the forth post-tumor implantation day and performed every other day on tail vein (total of 4 times). The injection dose of PEG-ZnPP was equivalent to 5 mg of ZnPP/kg (concentration of 1.75 mg/0.1 ml PBS).
In the second *in vivo* trial on Fischer rats (Group B), intravenous treatment with PEG-ZnPP was begun on the third post-tumor implantation day and performed every other day on tail vein (total of 4 times). In Group B, Fisher Rats received injections of PEG-ZnPP equivalent 7.5 mg/kg ZnPP/kg (concentration 1.75 mg/0.1 ml PBS). The intravenous treatment dose of PEG-ZnPP was based on the previous study of Fang *et. al* [72] and adjusted according to Equivalent Surface Area Dosage Conversion Factors [79]. For tail vein injection, rats were anesthetized with an intraperitoneal injection of 3mL/kg of a stock anesthesia solution with the same combination for tumor implantation. As the rats were anesthetized, they were positioned in a tail-first restrainer.

4.2.5. Neurological monitoring

Neurological motor scores applied for each extremity were measured daily after F98 glioma cell implantation on the Fisher rat group. This neurological scoring system, the Berlin Baltimore Brainstem (BBB) score previously described by Thomale *et al.* [13] (table 1), was applied. BBB is a modified scoring system used for cerebral ischemia [80, 81], which evaluates motor function of the extremities and each extremity can have a maximum value of four and a minimum value of zero. According to the scoring system, a total of 4 points for cases of complete plegia of one limb could be applied with possible additional 2 points for abnormal movement, such as tilted head to the side or axial body rotation [13]. However, the total possible score on the rating scale was not supposed to be reached, because rats that scored 14 points and above were euthanized according to the experimental protocol to avoid any extreme suffering of the animals.

The neurological monitoring for the motor abilities of the rats was carried out on a secured surface measuring 120 cm x 90 cm. Each rat was observed long enough until neurological scoring of each extremity was clearly determined.

Motor Score	0	No deficit
	1	Able to walk with slight asymmetry Decreased resistance when pushed from the contralateral side
	2	Walk with obvious asymmetry
	3	Slight movement present, with no use for walking
	4	No movement
Points added for abnormal movement	1	Tilted head to the side
	2	Axial body rotation
Total score	0-18	

Table 1. Berlin-Baltimore brainstem neuro-score [13]

4.2.6. Weight Measuring

As weight loss characterizes the morbidity status of cancer [82], the weight changes of rats over time were measured daily. This measurement was carried at the rat housing room.

4.3. Statistical Analysis

Analysis and calculations were performed using Prism 7 GraphPad software (Prism, CA, USA). Results are expressed as means ± standard error of mean (SEM), or as stated otherwise.

To calculate the value of the test statistic (p-values) of *in vitro* studies, weight changes and neurological changes, the Mann-Whitney-U-Test, one of the nonparametric tests, was applied, as this test compares the means of outcomes of two independent groups (control group vs. treated group), with the assumption of the data not being normally distributed. The two- tailed p value was applied, as there is no previous data regarding the efficacy of PEG-ZnPP on glioma cell lines.

For survival analysis, the logrank test (Mantel-Cox method) [83], which is the most commonly used method for comparing the survival distributions of two groups, was applied. This logrank test is used to test the null hypothesis with no differences in survival event, which is the events of death, between two or more independent groups [83]. The survival curves were created using Prism 7 GraphPad software (Prism, CA, USA). By conventional criteria, p-values of less than 0.05 are considered significant.

5. Results

5.1. In Vitro

5.1.1. Effect of PEG-ZnPP on Rat Glioma Cells: Anti-Proliferation

To assess the potential anti- proliferative effects of PEG-ZnPP on rat glioma cell growth, the proliferation assays of C6 and F98 glioma cell lines were performed and evaluated by counting cell numbers after treating with 40 µM PEG-ZnPP or PBS. Results show that the control group and the group treated with PEG-ZnPP show continuous proliferation of both glioma cell lines (Table 2 and Table 3). However, in the group with PEG-ZnPP treatment the cell numbers in the F98 cancer cell line were significantly decreased compared with control (*p<0.05, PEG-ZnPP vs. Ctrl, n = 4; figure 3). F98 glioma cell lines revealed profound growth inhibition under the influence of PEG-ZnPP. This significant inhibition of proliferation in PEG-ZnPP added cultures was seen at day six after treatment (figure 3B). F98 cells seemed more sensitive to PEG-ZnPP treatment.

		Cell Counts of C6 cell lines	
Day	n	Control	Treated
0	4	25000	25000
2	4	353137,5±38387,8	293562,5±43091,28
4	4	1814025±187503,57	1285725±277396,48
6	4	10700825±1453804,15	7074031,25±1230657,81

Table 2. The proliferation assay was performed a total of 4 times. (values are given as mean ± standard error of mean), Control group vs. treatment group of C6 cell lines (n=4). P-values are calculated via Mann-Whitney U Test Calculator (two-tailed)

		Cell Counts of F98 cell lines	
Day	n	Control	Treated
0	4	25000	25000
2	4	208000±17813,85	208000±23352,37
4	4	1090250±120901,04	847475±156324,49
6	4	5020275±557290,24	2585650±463360,06*

Table 3. The proliferation assay was performed a total of 4 times. (values are given as mean ± standard error of mean), Control group vs. treatment group of F98 cell lines (n=4). P-values are calculated via Mann-Whitney U Test Calculator (two-tailed)

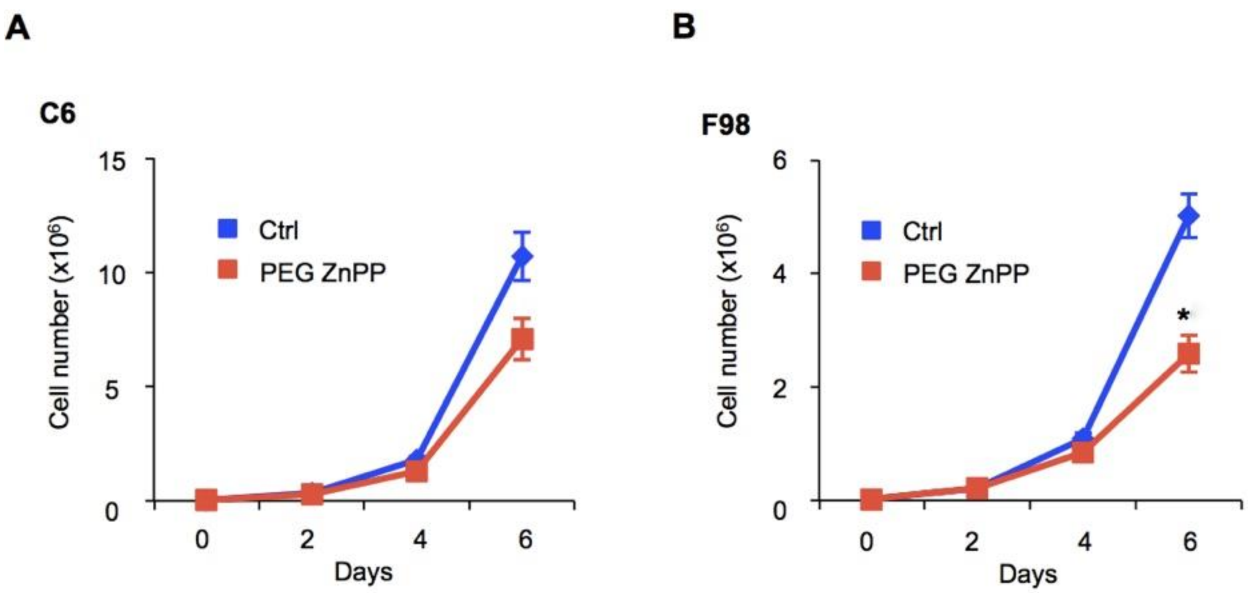

Figure 3. PEG-ZnPP inhibits rat glioma cell proliferation

F98 and C6 glioma cells were seeded at a density of 2.5x10[4]cells/well and grown for up to six days. In them, 40μM PEG-ZnPP or PBS (Lonza, USA) as a vehicle was added. Day 0: cell number: (2.5x10[4]). (A) Proliferation assay performed with C6 cells showing at day six after treatment a decrease in cell number compared to vehicle-treated cells. (B) Proliferation assay performed with F98 cells showing at day six after treatment a significant decrease in cell number compared to vehicle-treated cells. Data are mean ± SEM *p<0.05, PEG-ZnPP vs. Control, n=4. P-values are calculated via Mann-Whitney U Test Calculator (two-tailed)

5.2. In Vivo

Systemic treatment with PEG-ZnPP did not show efficacy in the brain stem model.

Based on our *in vitro* results, particularly the inhibition of proliferation in response to PEG-ZnPP treatment, we performed *in vivo* experiments to evaluate the anticancer therapeutic efficacy of PEG-ZnPP.

5.2.1. Weight changes

In the Group A Sprague Dawley rats, body weight increased until the 16th postoperative day in both groups with treatment and without treatment. Weight gain in the control group was more pronounced than in the group with treatment, which showed significant differences at days 6, 8, 10, 12, 14 and 16.

In the Group B Fischer rats with PEG-ZnPP treatment, body weight remained stable before it begun to decrease between 15th and 17th postoperative days. In control rats, an early weight gain was observed followed by a weight loss, which occurred earlier than in the PEG-ZnPP group and was significantly different at days 5, 9, 11, and 13. (table 2).

	Sprague Dawley rats body weight changes [g]									
Days	2	6	8	10	12	14	16	18	21	
CG	373.1±24	383.8±21	393.1±17	399.4±18	402.5±19	409.4±18	418.1±19	413.1±25	392.1±38	
TG	368.3±37	350.6±31*	350.6±31*	355±30*	360±28*	370±31*	385.7±39*	385.6±44	371.9±60	
	Fisher rats body weight changes [g]									
Days	3	5	7	9	11	13	15	17	19	21
CG	152.5±8	162.5±8	161.7±8	161.7±9	162.5±8	162.5±8	156.7±11	147.5±15	138±19	131.3±14
TG	149.4±11	150±10*	152.8±9	144.3±7*	145±10*	146.4±7*	147.1±10	142.9±13	132±14	121±5

Table 2. Weight changes (values are given as mean ± standard deviation). CG: Control group, TG: Therapy group (* $p<0.05$). P-values are calculated via Mann-Whitney U Test Calculator (two-tailed)

5.2.2. Neurological monitoring.

Neurological changes were monitored in Fischer rats (group B). In the control group, neurological deficits began to occur from day 15. In the treatment group, they occurred from the day 17. During this period, weight loss was also progressive. Once the neurological deficits began to occur, a progressive worsening of neurological performance was observed without any significant differences among the groups (Table 3). As the total score reached 14 points for an individual rat (maximal possible score: 18 [13]), rats were euthanized according to the experimental protocol.

Days	3	5	7	9	11	13	15	17	19	21
CG	0±00	0±00	0±00	0±00	0±00	0±00	0.17±0.4	2.17±2.3	5.8±4.5	5.8±4.6
TG	0±00	0±00	0±00	0±00	0±00	0±00	0±00	2.7±3.2	2.6±1.8	6.2 ±2.6

Table 3. Neuroscore changes of Fischer rats (values are given as mean ± standard deviation). CG: Control group, TG: Therapy group. (* p<0.05). P-values are calculated via Mann-Whitney U Test Calculator (two-tailed)

5.2.3. Survival Rate

No difference in overall survival between the group with intravenous PEG-ZnPP therapy versus control group was observed (Figure 6). In the group A Sprague Dawley rats with PEG-ZnPP treatment, the median survival was 23 days (range: 21-49 days). Control rats without therapy had a median survival of 24 days (range: 20-48 days; p = 0.47; log-rank test).

In the group B with Fisher rats, used in the second experiment, median survival of rats was 22 days (range: 9-26 days) with therapy, versus 22.5 days (range: 29-25 days) without therapy (p = 0.73; log-rank test). There were no differences of survival periods between the groups with therapy and without therapy.

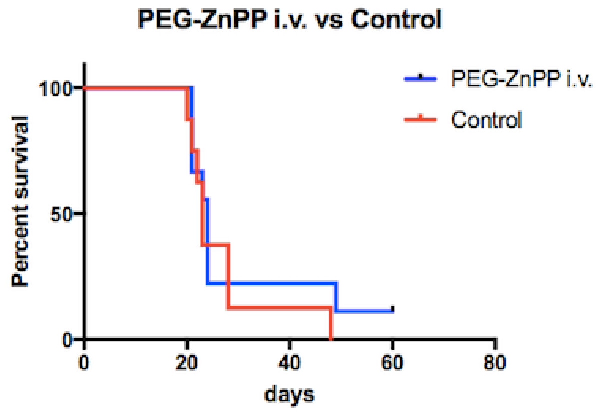

Figure 6A. Survival curves for group A with Sprague Dawley rats

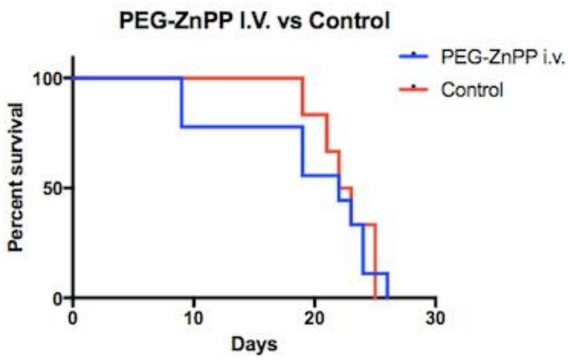

Figure 6B. Survival curves for group B with Fischer rats

Fig. 6. Survival rates of brainstem tumor models after intravenous treatment with PEG-ZnPP (A) Group A with PEG-ZnPP via I.V. in Sprague Dawley rats, male (C6 cells implanted): Dose: equivalent 5 mg of ZnPP/kg, Concentration 1.75 mg/0.1 ml PBS, Control: 8 rats, Therapy: 9 rats. Intravenous treatment was performed on days 4, 6 and 7 after tumor implantation. The median survival of rats with the PEG-ZnPP, 23 days (range: 21-49 days (1= Censored subject)); rats as control, 24 days (range: 20-48 days), P=0.47; log-rank test

(B) Group B with PEG-ZnPP via I.V. in Fischer rats (F98 cells implanted): Dose: equivalent 7.5 mg/kg ZnPP/kg. Concentration 1.75 mg/0.1 ml PBS, Average weight = 143.7 g, Control: 6 rats, Therapy: 9 rats. On 3, 5, 7 and 9 post-tumor implantation days, intravenous treatment was performed. The median survival of rats with the PEG-ZnPP: 22 days (range: 9-26 days); rats as control, 22.5 days (range: 19-25 days), P=0.73; log-rank test

6. Discussion

Since the potent anticancer effect of ZnPP appeared to be promising, several studies have been carried out investigating preclinical and clinical application of ZnPP, which was somewhat restricted due to lack of water solubility. However, as Sahoo *et al.* developed the conjugated ZnPP, PEG-ZnPP, ZnPP achieved water solubility by micelle formation [52]. The PEG-part contributes to forming an aqueous layer on the compounds, so that the pegylated ZnPPs are safe from early blood clearance and PEG-ZnPP achieves increased circulation time, as this compound behaves like macromolecules [84]. The benefits of pegylation include not only the water solubility, but also similar anticancer effects to ZnPP, and the character of macromolecule due to its molecular weight of about 68,000; this character contributes to the EPR effect. Several experimental studies have demonstrated that PEG-ZnPP could be considered as a promising anticancer agent due to its potential effects against various tumors [52, 72, 85]. To our knowledge, so far there was no study investigating a potential efficacy of PEG-ZnPP on glioma cells, F98 and C6 *in vitro* and *in vivo*.

6.1. Inhibition of Rat Glioma Cell Proliferation by PEG-ZnPP

6.1.1. Effect of PEG-ZnPP via Apoptosis

In this present study, we investigated if PEG-ZnPP inhibits proliferation of rat glioma cells. Several studies proved the anticancer efficacy of PEG-ZnPP on tumor cells, including colon cancer and leukemic cells *in vitro* [72, 86]. Significant anti-proliferative activity of PEG-ZnPP in F98 glioma cell lines was found on day 6 in the present study. In order to explain the inhibition of proliferation, further *in vitro* studies, such as assessment of cell cycle and apoptosis, may be needed.

Buttke and Sandstrom [87] reported that oxidative stress may be a potential mediator of apoptosis induction. The anti-inflammatory properties of HO-1 are due to its ability to degrade heme und generate bilirubin, free iron and carbon monoxide [16]. HO-1 plays a pivotal role for modulating inflammation by producing bilirubin, which protect cells from apoptosis. Bilirubin is one of the most abundant endogenous antioxidants in mammalian tissues and accounts for most of the antioxidant activity in human serum [40] and shows scavenging activity against various oxidants including superoxide, peroxyradical, and peroxynitrite [40, 41].

Apoptosis, also referred to as programmed cell death, is a vital process which enables an organism to maintain homeostatic cell status by eliminating cells. This process also may occur as a defence mechanism for example, as immune reactions or when cells are damaged by toxic agents [88]. There are studies reporting the cytoprotective effect of HO-1 via anti-apoptotic effect in transplant injury during organ rejection, so that induction of HO-1 may protect cells from chronic inflammatory reactions [89, 90]. Increased expression of HO-1 is inevitable for long term survival after transplantation [90]. This suggests that the inhibition of HO activity makes tumor cells more susceptible to ROS [91, 92]. The cytotoxic effect of ZnPP and PEG-ZnPP due to specific inhibition of HO-1 can trigger the apoptotic pathway via caspase-3 cascade [72]. Tananka *et al.* reported enhanced caspase-3 activity in ZnPP treated hepatoma cells [53]. In addition, there are studies that NO, which is produced in excess during solid tumor growth, inhibits apoptosis via inhibition of the caspase protease cascade [93, 94]. Caspases appears as inactive procaspase that usually require dimerization and cleavage for further activation. Caspase-3 is known as an essential enzyme for apoptosis, which is activated by capase-8 in the extrinsic pathway or casepase-9 in the intrinsic pathway [95]. Extrinsic apoptosis is induced by extracellular ligands binding to death receptors and intrinsic apoptosis occurs due to factors released from the mitochondria, so that it is also known as mitochondrial apoptosis [95]. Via both pathways the caspase-3 can be activated and the apoptosis is triggered.
HO-1 inhibition also causes enhanced transcription of p53 [96], which induces genes encoding the pro-apoptotic transcriptional target gene including, Bax, Puma, Noxa and Perp to activate the apoptotic pathway [97] .
Tanaka *et al.* [53] used a siRNA to supress the expression of HO-1 incultured in a cell line of human colon adenocarcinoma, treating with ZnPP IX, in which antiapoptotic activity of HO-1 was confirmed.

6.1.2. Effect of PEG-ZnPP on the Cell Cycle

Additionally, assessment of the effect of PEG-ZnPP on the cell cycle phase can be investigated. ZnPP can cause inhibition of hematopoesis in bone marrow, which may suggest that ZnPP could alter the cell cycle by inhibiting HO-1 [98]. HO-1 inhibition by administering ZnPP causes enhanced transcription of p53 [96], which plays a critical role in tumor supression. In various stress environments p53 protein, also referred to as cellular tumor antigen p53 and tumor suppressor p53, is responsible for regulating a set of its target genes and initiates stress responses including cell cycle arrest and apoptosis to execute tumor suppression [99, 100]. P53 induces the expression of p21, also known as cyclin-dependent kinase inhibitor 1 (CKI), which may cause apoptosis and cell cycle arrest by inhibiting cyclin/CdK complexes [101]. Active cyclin/CdK complexes inactivate members of the retinoblastoma protein (Rb) family by phosphylating it [102, 103]. Rbs are negative regulators of G1 and S-phase progression, which causes continuous cell cycle progression [102, 103]. CKIs can inhibit the activity of cyclin/CdK complexes so that the cell cycle progression can be negatively regulated [102, 103]. Yang *et al.* proved that the induction of p53 occurred depending on dose of ZnPP [96]. This may suggest that the p53 induction causes the arrest of G1 phase by inducing the expression of p21. Further experiments are required to determine the time course of the different processes occurring in our cells in response to PEG-ZnPP treatment, but we can speculate that PEG-ZnPP inhibits F98 and C6 glioma cell proliferation through the induction of cell cycle arrest, which could precede cell death processes.

6.2. EPR Effect

Pharmacokinetic study by Fang *et al.* [72] detected the increased amount of PEG-ZnPP biocompatible macromolecules in tumor tissue in a time-dependent manner. In addition, these macromolecules were decreased in systemic circulation gradually [72]. Increased size of molecule contributes to accumulation in tumor according to the EPR effect [68]. This tumor-specific accumulation of biocompatible macromolecules and lipids after systemic administration is due to its capacity to escape from renal clearance [68-71, 104]. PEG-ZnPPs have a molecular size larger than 40,000, i.e., large enough to meet this criterion.

6.3. Antitumor Efficacy of PEG-ZnPP in vivo

Based on the *in vitro* effect of PEG-ZnPP on proliferation and glioma cell death data, we investigated *in vivo* antitumor efficacy in rat glioma brainstem models. In contrast to our *in vitro* studies, no survival benefit of systemic therapy with PEG-ZnPP on rat glioma brainstem model was proven. To achieve an appropriate administering systemic dose of PEG-ZnPP, we have set up the initial dosage based on a previous study [72] and modified by equivalent surface area dosage conversion factors [79]. When it was given systemically, the adverse effect and toxicity of PEG-ZnPP were minor as all rats tolerated even the higher dosage of PEG-ZnPP well (from PEG-ZnPP equivalent 5 mg of ZnPP/kg to PEG-ZnPP equivalent 7.5 mg of ZnPP/kg). Higher dosage of PEG-ZnPP can be administered more than 3 times a week to achieve its maximal therapeutic dose. We speculate that the administered dose was close to maximum, which it may have reached. However, it might not be a matter of dosage or concentration but this particle may have difficulties to be delivered directly to brain tumor cells.

Two main factors for the failure of chemotherapy in treatment of CNS tumors include natural or acquired resistance to chemotherapy expressed by tumor cells, and restricted delivery due to the blood-brain barrier (BBB) [105]. As the efficacy of PEG-ZnPP was confirmed in the present study, we speculate that the reason for failure of the systemic therapy is the inability of the substance to sufficiently cross the BBB. The impact of the BBB on chemotherapy is still controversial. However, it has been regarded that BBB is the main factor in the impaired efficacy of chemotherapy. The efficacy of chemotherapeutics in the treatment of brain tumor is often hampered due to the BBB.

6.3.1. Brain-Blood Barrier

Various chemical signals including neurotransmitters and modulators, and electrical signals including synaptic potentials and action potentials, which are inevitable for cell-to-cell communication, require their own microenvironment, which protects the brain from variations in the blood. The BBB is necessary to provide an optimal environment for brain function. The BBB is composed with endothelial cells (EC) that form the walls of the capillaries, and its basement membrane, which is adjoined by tight junction protein. The endothelial cells are the core anatomical unit of the BBB, which prevent the uncontrolled transport of water-soluble molecules between blood circulation system and brain parenchyma [106]. Pericytes and astroglial foot processes of astrocytes surround the ECs. These ECs are connected via adherent junctions, tight junctions and gab junctions. Tight junctions and adherent junctions underlie the physical barrier that impedes paracellular diffusion of ions, macromolecules and other polar solutes [107].

Potential routes across the BBB for drugs and other solutes include passive diffusion, which is driven by concentration gradient, mainly for small hydrophobic therapeutics[108]. Most drugs which can cross the BBB, diffuse through membranes [109]. Other routes include carrier mediated efflux for glucose, amino acids and nucleosides [108], and tight junction modulation [110]. Non-polar solutes and lipid solubles may cross the BBB by passive diffusion and small peptides can transport the BBB via carrier mediate influx [110]. Polar solutes can cross via tight junction modulation relaxing the junctions [110].

The normal BBB limits the permeation of ionized water-soluble compounds with a molecular weight > 180 daltons (D) [111]. Kroll *et al.* reported that most currently available effective chemotherapeutic agents have a molecular weight of 200-1200 D [112]. Pardridge reported [113] that almost all small drugs which are permeable to BBB are lipid soluble molecules with a weight less than 400 D [113]. A pharmacokinetic study confirmed that elution time of PEG-ZnPP was comparable to that of bovine serum albumin (67 kDa), which suggests that PEG- ZnPP behaves as large as BSA in an aqueous system [52].

Drugs which can cross the BBB via diffusion show the following characters: a low molecular weight and lipophilicity. However, drugs taken up into membranes must have the capability to reach to the target after crossing the BBB to exert a therapeutic effect of anticancer. The character of lipid solubility may contribute to success in crossing the BBB, however, it can be easily sequestered by the capillary bed and not reach the target [114]. Therefore, the drugs should meet at least two criteria: they should have characters which can cross the BBB and reach the tumor after crossing the BBB. These are the prerequisites for the success of systemic chemotherapy for CNS malignancy. The hydrophilic property of PEG-ZnPP, which is gained due to conjugation with the PEG-chain [52] can be regarded as another additional limitation to crossing the BBB. However, the lipophilicity of substance as a benefit for crossing the BBB applies to small drugs, which can cross the BBB via diffusion.

6.3.1.1. Transport of Macromolecules

Transport of macromolecules requires both specific and nonspecific interaction between macromolecules and receptors expressed on the luminal and the abluminal surfaces of the brain capillary endothelial cells [115]. Endocytosis and transcytosis play an important role for macromolecues [115]. Endocytosis is a type of active transport on which a cell transports different compounds into itself by forming vesicles. When compounds and macromolecules are expelled into the other side, it is termed as transcytosis [115]. Adsorptive-mediated transcytosis (AMT) and receptor-mediated transcytosis (RMT) are the main vesicular mechanism for large molecules to cross the brain endothelium [116]. In the AMT pathway, positively charged peptides interact with the negatively charged membrane surface, so that membranes can be invaginated via forming vesicles [117]. RMT systems are selective pathways to cross the BBB through the initial binding of a ligand to receptor-mediated RMT receptors. The RMT pathway is known as a favourable delivery pathway for toxic agents. Generally, transporting macromolecules via tight junction is not possible [115].

Even though the BBB is often regarded as a main factor of failure of chemotherapy in CNS, we must acknowledge that there is objection to the fact that the integrity of the BBB in the center of malignant brain tumors is disturbed [105]. This leaky BBB is heterogeneous [105], variable and dependent on the tumor type and size [112]. Even though the BBB of malignant glioma is interrupted and fenestrated for unimpeded passage of low molecular weight particles [118], such endothelial disruption due to discontinuities of endothelial cells of tumor microvessels may not be wide enough for the effective passage of PEG-ZnPP particles and to achieve therapeutic efficacy.

Another explanation, which may limit the systemic chemotherapeutic efficacy, is the “sink effect” [119] . The hydrostatically driven flow of CSF, which begins from ventricles via subarachnoid space to venous blood, contributes to a strong diffusion gradient to lower ECF metabolites and catabolites being produced by parenchymal cells in brain [120]. This capacity to lower the “steady state” of drugs [119] delivered to the CNS, may also contribute to a diminished chemotherapeutic concentration and lead to therapy failure in CNS tumor [112].

6.4. Alternative Approach

So far, we have to admit that as long as solutions to the BBB problem are not found, there are only few effective treatments for CNS malignancies including brainstem tumors. PEG-ZnPP may have a limited penetrance to the BBB, however, it could still represent a potential agent against brainstem tumor, if the compound could be locally delivered to its targeted localization. Currently a lot of research is on-going in the field of nanoparticles to overcome this obstacle by enhancing PEG-ZnPP bioavailability. Local delivery of antitumor therapeutic agents into the brain allows compounds to bypass the BBB. The bulk-flow properties of convection enhanced delivery (CED) contributes to a relatively homogeneous concentration of large molecules [121, 122]. The compounds, which do not readily penetrate the BBB from the systemic circulation when they are delivered by convection enhanced delivery, remain sequestered on the abluminal side of the BBB within the perfused parenchyma for prolonged periods, until they are metabolized and cleared from the interstitial spaces [123-126]. These compounds do not readily leak through the CNS blood vasculature in CNS and into the systemic circulation. There are studies which demonstrated the possible use of CED in a rat brain stem model [127, 128]. Further investigations are clearly required to clarify that local delivery of PEG-ZnPP is technically possible, and the toxicity effect of PEG-ZnPP on normal brain and tumor *in vivo* studies.

7. Conclusion

The present *in vitro* study proved that PEG-ZnPP, a specific inhibitor of HO-1, has a potential antitumor effect against glioma cell lines including C6 and F98. However, despite its anti-proliferative efficacy via enhanced activity of apoptosis on glioma cells, no survival benefit in the rat brainstem glioma model was observed in the in-vivo experiments. We speculate that it is mainly due to limited permeability of PEG-ZnPP through the BBB into the tumor. For the clinical application of PEG-ZnPP, further investigation should be guaranteed to find better approaches to deliver the PEG-ZnPP into the brainstem glioma in the rat model.

8. Reference

[1] Frazier JL, Lee J, Thomale UW, Noggle JC, Cohen KJ, Jallo GI (2009) Treatment of diffuse intrinsic brainstem gliomas: failed approaches and futures strategies. Journal of Neurosurgery: Pediatrics 3: 259-269

[2] Hargrave D, Bartels U, Bouffet E (2006) Diffuse brainstem glioma in children: critical review of clinical trials. Lancet Oncol 7: 241-248

[3] Barkovich AJ, Krischer J, Kun LE, Packer R, Zimmerman RA, Freeman CR, Wara WM, Albright L, Allen JC, Hoffman HJ (1990) Brain stem glioma: a classification system based on magnetic resonance imaging. Pediatric Neurosurgery 16: 73-83

[4] McCrea HJ, Souweidane MM (2013) 43. Brainstem Gliomas. In: Conerly K (ed) Principles and Practice of Pediatric Neurosurgery, 3rd edn. Thieme, New York, pp 553-562

[5] Lin TF, Prados M (2017) Pediatric CNS Tumors. Springer International

[6] Albright AL (1996) Diffuse brainstem tumors: when is a biopsy necessary? Pediar Neurosurg 24: 252-255

[7] Epstein F, Wisoff J (1988) Intrinsic brainstem tumors in childhood, surgical indications. . J Neurooncol 6: 300-317

[8] Cohen KJ, Jabado N, Grill J (2017) Diffuse intrinsic pontine glioma- current management and new biologic insights. Is there a glimmer of hope? Neuro-Oncology

[9] Walker DA, Punkt JAG, Sokal M (2004) Brainstem tumors. In Walker DA, Perlongo G, Punt JAG, Tayor RE eds. Brain and Spinal tumors of childhood. . Arnold

[10] Smith MA, Freidlin B, Ries LA, Simon R (1998) Trends in reported incidence of primary malignant brain tumors in children in the United States. J Natl Cancer Inst 90: 1269-1277

[11] Khatua S, Moore KR, Vats TS, Kestle JR (2011) Diffuse intrinsic pontine glioma- current status and future strategies. Childs Nerv System 27: 1391-1397

[12] Jallo GI, Volkov A, Wong C, Carson Sr BS, Penno MB (2006) A novel brainstem tumor model: functional and histopathological characterization. Childs Nerv Syst 22: 1519–1525

[13] Thomale UW, Tyler B, Renard V, Dorfman B, Chacko VP, Carson BS, Haberl EJ, Jallo GI (2009) Neurological grading, survival, MR imaging, and histological evaluation in the rat brainstem glioma model. Childs Nerv Syst 25: 433-441

[14] Jallo GI, Penno M, Sukay JY, Liu B, Tyler J, Carson BS, Guarnieri M (2005) Experimental models of brainstem tumors : development of a neonatal rat model. Childs

Nerv Syst 21: 399-403
[15] Maines MD (1988) Heme oxygenase function, multiplicity, regulatory mechanisms, and clinical applications. FASEB Journal 2: 2557-2568
[16] Maines MD (1997) The Heme Oxygenase System: A Regulator of Second Messenger Gases. Annu Rev Pharmacol Toxicol 37: 517-554
[17] Schacter BA (1988) Heme catabolism by heme oxygenase: Physiology, regulation, and mechanism of action. Semin Hematol 25: 349-369
[18] Tenhunen R, Marver HS, Schmid R (1968) The enzymatic conver- sion of heme to bilirubin by microsomal heme oxygenase. Proc Natl Acad Sci 61: 748–755
[19] Jozkowicz A (2007) Was Heme oxygenase-1 in tumors: is it a false friend? . Dulak Antioxd Redox Signal 9: 2099-2117
[20] Snyder SH, Baranano DE (2001) Heme oxygenase: a font of multiple messengers. Neuropsychopharmacology 25: 294-298
[21] Stocker R, Yamamoto Y, McDonagh AF, Glazer AN, Ames BN (1987) Bilirubin is an antioxidant of possible physiological importance. Science 235: 1043-1046
[22] McCcoubrey WKJ, Huang TJ, Maines MD (1997) Isolation and Characterization of a cDNA from the Rat Brain that Encodes Hemoprotein Heme Oxygenase-3. Eur J Biochem 247: 725-732
[23] Trakshel GM, Kutty RK, Maines MD (1988) Resolution of the rat brain heme oxygenase activity: absence of a detectable amount of the inducible form (HO-1). Arch Biochem Biophys 260
[24] Takeda A, G. P, Abraham NG, Dwyer BE, Kutty RK, Laitinen JT, Petersen RB, Smith MA (2000) Overexpression of Heme Oxygenase in Neuronal Cells, the Possible Interaction with Tau The Journal of Biological Chemistry 287: 5395-5399
[25] Shibahara S (1988) Regulation of heme oxygenase gene expression. Semin Hematol 25: 370-376
[26] Keyse SM, Tyrrell RM (1989) Heme oxygenase is the major 32-kDa stress protein induced in human skin fibroblasts by UVA radiation, hydrogen peroxide, and sodium arsenite. Proc Natl Acad Sci USA 86: 99-103
[27] Mitani K, Fujita H, Fukuda Y, Kappas A, Sassa S (1993) The role of inorganic metals and metalloporphyrins in the induction of haem oxygenase and heat-shock protein 70 in human hepatoma cells. Biochem J 290: 819-825
[28] Motterlini R, Foresti R, Bassi R, Calabrese V, Clark JE, Green CJ (2000) Endothelial heme oxygenase-1 induction by hypoxia. Modulation by inducible nitric

oxide synthase and S-nitrosothiols. J Biol Chem 275: 13613-13620
[29] Doi K, Akaike T, Fujii S, Tanaka S, Ikebe N, Beppu T, Shibahara S, Ogawa M, Maeda H (1999) Induction of haem oxygenase-1 nitric oxide and ischaemia in experimental solid tumours and implications for tumour growth. Br J Cancer 80: 1945-1954
[30] Valaes T, Petmezaki S, Henschke C, Drummond GS, Kappas A (1994) Control of jaundice in preterm newborns by an inhibitor of bilirubin production: Studies with tinmesoporphyrin. Pediatrics 93: 1-11
[31] Santoro MG (2000) Heat schock factors and the control of the stress response. Biochem Parm 59: 55-63
[32] Pae HO, Oh GS, Choi BM, Chae SC, Chung HT (2003) Differential expression of heme oxygenase-1 in CD25- and CD25+ subsets of human CD4 T cells. Biochem Biophys Res Commun 306: 701-715
[33] Otterbein LE, Bach FH, Alam J, Soares M, Tao LH, Wysk M, Davis RJ, Flavell RA, Choi AM (2000) Carbon monoxide has anti- inflammatory effects involving the mitogen-activated protein kinase pathway. Nat Med 6: 422-428
[34] Was H, Cichon T, Smolarczyk R, Rudnicka D, Stopa M, Chevalier C, Leger JJ, Lackowska B, Grochot A, Bojkowska K, Ratajska A, Kieda C, Szala S, Dulak J, Jozkowicz A (2006) Overex- pression of heme oxygenase-1 in murine melanoma: increased proliferation and viability of tumor cells, decreased survival of mice. Am J Pathol 169: 2181-2198
[35] Chen GG, Liu ZM, Vlantis AC, Tse GM, Leung BC, van Hasselt CA (2004) Heme oxygenase-1 protects against apoptosis by tu- mor necrosis factor-alpha and cycloheximide in papillary thyroid carcinoma cells. J Biochem 92: 1246-1256
[36] Mayerhofer M, Florian S, Krauth MT, Aichberger KJ, Bilban M, Marculescu R, Printz D, Fritsch G, Wagner O, Selzer E, Sperr WR, Valent P, Sillaber C (2004) Identification of heme oxygenase- 1 as a novel BCR/ABL-dependent survival factor in chronic myeloid leukemia. Cancer Res 64: 3248-3254
[37] Liu ZM, Chen GG, Ng EK, Leung WK, Sung JJ, Chung SC (2004) Upregulation of heme oxygenase-1 and p21 confers resistance to apoptosis in human gastric cancer cells. . Oncogene 23: 503-513
[38] Busserolles J, Megiasd J, Terencio MC, Alcaraz MJ (2006) Heme oxygenase-1 inhibits apoptosis in Caco-2 cells via activation of Akt pathoway. Int J Biochem Cell Biol 38: 1510-1517

[39] Farrera J-A, Jauma A, Ribo JM, Peire MA, Parellada PP, Roques-Choua S, Bienvenue E, Seta P (1994) The antioxidant role of bile pigments evaluated by chemical tests. Bioorganic & Medicinal Chemistry 2: 181-185

[40] Minetti M, Mallozzi C, Di Stasi AMM, Pietraforte D (1998) Bilirubin is an effective antioxidant of peroxynitrite-mediated protein oxidation in human blood plasma. Arch Biochem Biophys 352: 165-174

[41] Dore S, Takahashi M, Ferris CD, Zakhary R, Hester LD, Guastella D, Snyder SH (1999) Bilirubin, formed by activation of heme oxygenase-2, protects neurons against oxidative stress injury. Proc Natl Acad Sci USA 96: 2445-2450

[42] Maines MD, Abrahamsson PA (1996) Expression of heme oxygenase-1 (HSP32) in human prostate: normal, hyperplastic, and tumor tissue distribution. Urology 47: 7270733

[43] Duckers HJ, Boehm M, True AL, Yet SF, San H, L. PJ, Clinton WR, Lee ME, Nabel GJ, Nabel EG (2001) Heme oxygenase-1 protects against vascular constriction and proliferation. Nat Med 7: 693-698

[44] Berberat PO, Dambrauskas Z, Gulbinas A, Giese T, Giese N, Künzli B, Autschbach F, Meuer S, Büchler MW, Friess H (2005) Inhibition of heme oxygenase-1 increases responsiveness of pancreatic cancer cells to anticancer treatment. Clin Cancer Res 15: 3790-3798

[45] Schacter BA, Kurz P (1982) Alterations in hepatic and splenic microsomal electron transport system components, drug metabolism, heme oxygenase activity, and cytochrome P-450 turnover in Murphy-Sturm lymphosarcoma-bearing rats. Cancer Res 42: 3557-3564

[46] Goodman AI, Choudhury M, da Silva JL, Schwartzman ML, Abraham NG (1997) Overexpression of the heme oxygenase gene in renal cell carcinoma. Proc Soc Exp Biol Med 214: 54-61

[47] Torisu-Itakura H, Furue M, Kuwano M, Ono M (2000) Co-expression of thymidine phosphorylase and heme oxygenase-1 in macrophages in human malignant vertical growth melanomas. Jpn J Cancer Res 91: 906-910

[48] McAllister SC, Hansen SG, Ruhl RA, Raggo CM, DeFilippis VR, Greenspan D, Früh K, Moses AV (2004) Kaposi sarcoma-associated herpesvirus (KSHV) induces heme oxygenase-1 expression and activity in KSHV-infected endothelial cells. Blood 103: 3465-3473

[49] Tsuji MH, Yanagawa T, Iwasa S, Tabuchi K, Onizawa K, Bannai S, Toyooka H,

Yoshida H (1999) Heme oxygenase-1 expression in oral squamous cell carcinoma as involved in lymph node metastasis. Cancer Lett 138: 53-59
[50] Hara E, Takahashi K, Tominaga T, Kumabe T, Kayama T, Suzuki H, Fujita H, Yoshimoto T, Shirato K, Shibahara S (1996) Expression of heme oxygenase and inducible nitric oxide synthase mRNA in human brain tumors. Biochem Biophys Res Commun 224: 153-158
[51] Deininger MH, Meyermann R, Trautmann K, Duffner F, Grote EH, Wickboldt J, Schluesener HJ (2000) Heme oxygenase (HO)-1 expressing macrophages/microglial cells accumulate during oligodendroglioma progression. Brain Res 882: 1-8
[52] Sahoo SK, Sawa T, Fang J, Tanaka S, Miyamoto Y, Akaike T, Maeda H (2002) Pegylated Zinc Protoporphyrin: A Water-Soluble Heme Oxygenase Inhibitor with Tumor-Targeting Capacity. Bioconjugate Chem 13: 1031-1038
[53] Tanaka S, Akaike T, Fang J, Beppu T, Ogawa M, Tamura F, Miyamoto Y, Maeda H (2003) Antiapoptotic effect of haem oxygenase-1 induced by nitric oxide in experimental solid tumour. Br J Cancer 24: 902-909
[54] Johnson TM, Yu ZX, Ferrans VJ, Lowenstein RA, Finkel T (1996) Reactive oxygen species are downstream mediators of p53-dependent apoptosis. Proc Natl Acad Sci USA 93: 11848-11852
[55] Fang J, Akaike T, Maeda H (2004) Antiapoptotic role of heme oxygenase (HO) and the potential of HO as a target in anticancer treatment. Apoptosis 9: 27-35
[56] Schuler M, Bossy-Wetzel E, Goldstein JC, Fitzgerald P, Green DR (2000) p53 induces apoptosis by caspase activation through mitochondrial cytochrome c release. J Biochem 275: 7337-7342
[57] Cisowski J, Loboda A, Jozkowicz A, Chen S, Agarwal A, Dulak J (2005) Role of heme oxygenase-1 in hydrogen peroxide-induced VEGF synthesis: effect of HO-1 knockout. Biochem Biophys Res Commun 326: 670-676
[58] Suzuki M, Iso-o N, Takeshita S, Tsukamoto K, Mori I, Sato T, Ohno M, Nagai R, Ishizaka N (2003) Facilitated angiogenesis induced by heme oxygenase-1 gene transfer in a rat model of hindlimb ischemia. Biochem Biophys Res Commun 302
[59] Maines MD (1981) Zinc-protoporphyrin is a selective inhibitor of haem oxygenase activity in the neonatal rat. . Biochem Biophys Acta 673: 339-350
[60] Fang J, Greish K, Qin H, Liao L, Nakamura H, Takeya M, Maeda H (2012) HSP32 (HO-1) inhibitor, copoly(styrene-maleic acid)-zinc protoporphyrin IX, a water-soluble micelle as anticancer agent: In vitro and in vivo anticancer effect. Eur j Pharm

Biopharm 81: 540-547
[61] Drummond GS (1987) Control of heme metabolism by synthetic metalloporphyrins. Ann N Y Acad Sci 514: 87-95
[62] Carmeliet P, Jain RK (2000) Angiogenesis in cancer and other diseases. Nature 407: 249-257
[63] Gee MS, Procopio WN, Makonnen S, Feldman MD, Yeilding NM, Lee WM (2003) Tumor vessel development and maturation impose limits on the effectiveness of anti-vascular therapy. Am J Pathol 162: 183-193
[64] Tong RT, Boucher Y, Kozin SV, Winkler F, Hicklin DJ, Jain RK (2004) Vascular normalization by vascular endothelial growth factor receptor 2 blockade induces a pressure gradient across the vasculature and improves drug penetration in tumors. Cancer Res 64: 3731-3736
[65] Vaupel P, Fortmeyer HP, Runkel S, Kallinowski F (1987) Blood flow, oxygen consumption, and tissue oxygenation of human breast cancer xenografts in nude rats. Cancer Res 47: 3496-3503
[66] Branco-Price C, Zhang N, Schnelle M, Evans C, Katschinski DM, Liao D, Ellies L, Johnson RS (2012) Endothelial cell HIF-1α and HIF-2α differentially regulate metastatic success. Caner cells 21: 52-65
[67] Tang N, Wang L, Esko J, Giordano FJ, Huang Y, Gerber HP, Ferrara N, Johnson RS (2004) Loss of HIF-1alpha in endothelial cells disrupts a hypoxia-driven VEGF autocrine loop necessary for tumorigenesis. Cancer Res 6: 485-495
[68] Matsumura Y, Maeda H (1986) A new concept for macromolecular therapeutics in cancer chemotherapy: mech- anism of tumoritropic accumulation of proteins and the antitumor agent smancs. Cancer Res 46: 6387-6392
[69] Maeda H (2001) The enhanced permeability and retention (EPR) effect in tumor vasculature: the key rome of tumor-selective macromolecular drug targeting. Advances in Enzyme Regulation 41: 189-207
[70] Maeda H, Sawa T, Konno T (2001) Mechanism of tumor-targeted delivery of macromolecular drugs, including the EPR effect in solid tumor and clinical overview of the prototype polymeric drug SMANCS. . J Controlled Release 74: 47-61
[71] Maeda H (2001) SMANCS and polymer-conjugated macromolecular drugs: advantages in cancer chemotherapy. Adv Drug Deliv Rev 46: 169-185
[72] Fang J, Sawa T, Akaike T, Akuta T, Sahoo SK, Khaled G, Hamada A, Maeda H (2003) In vivo antitumor activity of pegylated zinc protoporphyrin: targeted inhibition of

heme oxygenase in solid tumor. Cancer Res: 3567-3574

[73] Fang J, Seki T, Maeda H (2009) Therapeutic strategies by modulating oxygen stress in cancer and inflammation. Adv Drug Deliv Rev 61: 290-302

[74] Fang J, Nakamura H, Iyer AK (2007) Tumor-targeted induction of oxystress for cancer therapy. J Drug Target 15: 475-486

[75] Wechsler H, Ramadan MA, Pfeiffer SE (1979) Morphologic and biochemical characteristics of transplantable neurogenic tumors induced by N-ethyl-N-nitrosourea in inbred BD IX rats. J Natl Cancer Inst 62: 811-817

[76] Barth RF (1988) Rat brain tumor models in experimental neuro-oncology: The 9L, C6, T9, F98, RG2 (D74), RT-2 and CNS-1 gliomas. J Neurooncol 36: 91-102

[77] Benda P, Lightbody J, Sato G, Levine L, Sweet W (1968) Differentiated rat glial cell strain in tissue culture. Science 161: 370-371

[78] Schmidek HH, Nielsen SL, Schiller AL, Messer J (1971) Morphological studies of rat brain tumors induced by N-nitrosomethylurea. J Neurosurg 34: 335-340

[79] Freireich EJ, Gehan EA, Rall DP, Schmidt LH, Skipper HE (1966) Quantitative comparison of toxicity of anticancer agents in mouse, rat, hamster, dog, monkey, and man. Cancer Chemother Rep 50: 219-244

[80] Zausinger S, Hungerhuber E, Baethmann A, Reulen H, Schmid- Elsaesser R (2000) Neurological impairment in rats after transient middle cerebral artery occlusion: a comparative study under various treatment paradigms. Brain Res 863: 94-105

[81] Bederson JB, Pitts LH, Tsuji M, Nishimura MC, Davis RL, Bartkowski H (1986) Rat middle cerebral artery occlusion: evaluation of the model and development of a neurologic examination. stroke 17: 472-476

[82] Dhanapal R, Saraswathi TR, Govind RN (2011) Cancer cachexia. J Oral Maxillofac Pathol 15: 257-260

[83] Bland JM, Altman DG (2004) The logrank test. BMJ 328: 1412

[84] Immordino ML, Dosio F, Cattel L (2006) Stealth liposomes: review of the basic science, rationale, and clinical applications, existing and potential. Int J Nanomed 297-315

[85] Fang J, Deng D, Nakamura H, Akuta T, Qin H, Iyer AK, Greish K, Maeda H (2008) Oxystress inducing antitumor therapeutics via tumor-targeted delivery of PEG-conjugated D-amino acid oxidase. Int J Cancer 122

[86] Cerny-Reiterer S, Meyer RA, Herrmann H, Peter B, Gleixner KV, Stefanzl G, Hadzijusufovic E, Pickl WF, Sperr WR, Melo JV, Maeda H, Jäger U, Valent P (2014)

Identification of heat shock protein 32 (Hsp32) as a novel target in acute lymphoblastic leukemia. Oncotarget 5: 1198-1211
[87] Buttke TM, Sandstrom PA (1994) Oxidative stress as a mediator of apoptosis. Immun Today 15: 7-10
[88] Norbury CJ, Hickson ID (2001) Cellular responses to DNA damage. Annu Rev Pharmaco Toxicol 41: 367-401
[89] Hancock WW, Buelow R, Sayegh MH, Turka LA (1998) Antibody-induced transplant arteriosclerosis is prevented by graft expression of anti-oxidant and anti-apoptotic genes. Nat Med 4: 1392-1396
[90] Soares MP, Lin Y, Anrather J, Csizmadia E, Takigami K, Sato K, Grey ST, Colvin RB, Choi AM, Poss KD, Bach FH (1998) Expression of heme oxygenase-1 can determine cardiac xenograft survival. Nat Med 4: 1073-1077
[91] Doi K, Akaike T, Horie H, Noguchi Y, Fujii S, Beppu T, Ogawa M, Maeda H (1996) Excessive production of nitric oxide in rat solid tumor and its implication in rapid tumor growth. Cancer (Phila) 77: 1598-1604
[92] Wu J, Akaike T, Maeda H (1998) Modulation of enhanced vascular permeability in tumors by a bradykinin antagonist, a cyclooxygenase inhibitor, and a nitric oxide scavenger. Cancer Res 58: 159-165
[93] Ogura T, DeGeorge G, Tatemichi M, Esumi H (1998) Suppression of antimicrotubule agent-induced apoptosis by nitric oxide: possible mechanism of a new drug resistance. Jpn J Cancer Res 89
[94] Mannick JB, Asano K, Izumi K, Kieff E, Stamler JS (1994) Nitric oxide produced by human B lymphocytes inhibits apoptosis and Epstein – Barr virus reactivation. Cell 79: 1137-1146
[95] McIlwain DR, Berger T, Mak TW (2013) Caspase Functions in Cell Death and Disease. Cold Spring Harbor Perspect Biol
[96] Yang G, Nguyen X, Ou J, Rekulapelli P, Stevenson DK, Dennery PA (2001) Unique effects of zinc protoporphyrin on HO-1 induction and apoptosis. Blood 97: 1306-1313
[97] Attardi LD, DePinho RA (2004) Conquering the complexity of p53. Nat Genet 36: 7-8
[98] Lutton JD, Abraham NG, Drummond GS, Levere RD, Kappas A (1997) Zinc protoporphyrins: potent in- 20. hibitors of hematopoieses in animal and human

bone marrow. Proc Natl Acad Sci U S A 94: 1432-1436
[99] Levine AJ, Hu W, Feng Z (2006) The p53 pathway: what questions remain to be explored? . Cell Death Differ 13: 1027-1036
[100] Vousden KH, Privies C (2009) Blinded by the light: the growing complixity of p53. Cell 137: 413-431
[101] Gartel AL, Tyner AL (2002) The Role of the Cyclin-dependent Kinase Inhibitor p21 in Apoptosis. Molecular Cancer Therapeutics 1: 639-649
[102] Sherr CJ (2000) The Pezcoller lecture: cancer cell cycles revisited. Cancer Res 60
[103] Sherr CJ, Roberts JM (1999) CDK inhibitors: positive and negative regulators of G1-phase progression. Genes Dev 13: 1501-1502
[104] Fang J, Sawa T, Maeda H (2003) Factors and mechanism of “EPR” effect and the enhanced antitumor effects of macromolecular drugs including SMANCS. Adv Exp Med Biol 519: 29-49
[105] Fortin D, Neuwelt EA (2003) Therapeutic manipulation of the blood barrier. Neurobase-neurosurgery. 1st ed. Medlink CD-ROM.
[106] Roberts RL, Fine RE, Sandra A (1993) Recepter-mediated endocytosis of transferrin at the blood-brain barrier. Journal of Cell Science 104: 521-532
[107] McConnell HL, Kersch CN, L. WR, Neuwelt EA (2017) The translational significance of the neurovascular unit J Biochem 292: 762-770
[108] Georgieva JV, Hoekstra D, Zuhorn IS (2014) Smuggling Drugs into the Brain: An Overview of Ligands Targeting Transcytosis for Drug Delivery across the Blood–Brain Barrier Pharmaceutics 6: 557-583
[109] Oldendorf WH (1974) Lipid solubility and drug penetration of the blood brain barrier. Proc Soc Exp Biol Med 147: 813-815
[110] Begley DJ, Brightman MW (2003) Structural and functional aspects of the blood-brain barrier. In L. Prokai, & K. Prokai-Tatrai (Eds.). Peptie Transport and Delivery into the Central Nervous System. Progress in Drug Research. Birkauser Verlag, Basel, Switzerland
[111] Fortin D, Desjardins A, Benji A, Niyonsega T, Boudrias M (2005) Enhanced chemotherapy delivery by intraarterial infusion and blood-brain barrier disruption in malignant brain tumors / The Sherbrooke experinece. Cancer 103: 2606-2615
[112] Kroll RA, Neuwelt EA (1998) Outwitting the blood-brain barrier for therapeutic purpose: osmotic opening and other means. Neurosurgery 42: 1083-1100

[113] Pardridge WM (2012) Drug transport across the blood-brain barrier. Journal of Cerebral Blood Flow & Methabolism 32: 1959-1972

[114] Banks WA (2009) Characteristics of compounds that cross the blood-brain. barrier. BMC Neurol 9: S3

[115] Xiao G, Gan LS (2013) Recepter mediated endocytosis and brain delivery of therapeutic biologics. International Journal of Cell Biology 2013: 1-14

[116] Hervé F, Ghinea N (2008) CNS delivery via adsorptive transcytosis AAPS J 10: 455-472

[117] Jones EM, Polt R (2015) CNS active O-linkes glycopeptide. Front Chem 3: 1-9

[118] Chertok B, Moffat BA, David AE, Yu F, Bergemann C, Ross BD, Yang VC (2008) Iron oxide nanoparticles as a drug delivery vehicle for MRI monitored magnetic targeting of brain tumors. Biomaterials 29: 487-496

[119] Brzica H, Abdullahi W, Ibbotson K, Ronaldson PT (2017) Role of Transporters in Central Nervous System Drug Delivery and Blood-Brain Barrier Protection: Relevance to Treatment of Stroke. Journal of Central Nervous System Disease 9: 1-12

[120] Perry MC (2008) The chemotherapy source book. Lipincott Williams & Wilkins USA

[121] Lieberman DM, Laske DW, Morrison PF, Bankiewicz KS, Oldfield EH (1995) Convection enhanced distribution of large molecules in gray matter during interstitial drug infusion. . J Neurosurg 82: 1021-1029

[122] Lonser RR, Corthesy ME, Morrison PF, Gogate N, Oldfield EH (1999) Convection enhanced selective excitotoxic ablation of the neurons of the globus pallidus internus for treatment of parkinsonism in nonhuman primates. J Neurosurg 91: 294-302

[123] Lonser RR, Walbridge S, Garmestani K, Butman JA, Walters HA, Vortmeyer AO, Morrison PF, Brechbiel MW, Oldfield EH (2002) Successful and safe perfusion of the primate brainstem: in vivo magnetic resonance imaging of macromolecular distribution during infusion. J Neurosurg 97: 905-913

[124] Bobo RH, W. LD, Akbasak A, Morrison PF, Dedrick RL, Oldfield EH (1994) Convection-enhanced delivery to macromolecules in the brain. Proc Natl Acad Sci U S A 91: 2076-2080

[125] Chen PY, T. O, Drummond DC, Kalra A, Fitzgerald JB, Kirpotin DB, Wei KC, Butowski N, Prados MD, Berger MS, Forsayeth JR, Bankiewicz K, James CD (2013) Comparing routes of delivery for nanoliposomal irinotecan shows superior anti-tumor activity of local administration in treating intracranial glioblastoma xenografts. Neuro

Oncol 15: 189-197
[126] Corem-Salkmon E, Ram Z, Daniels D, Perlstein B, Last D, Salomon S, Tamar G, Shneor R, Guez D, Margel S, Mardor Y (2011) Convection-enhanced delivery of methotrexate-loaded maghemite nanoparticles. Int J Nanomedicine 6: 1595-1602
[127] Thomale UW, Tyler B, Renard VM, Dorfman B, Guarnieri M, Haberl HE, Jallo GI (2008) Local chemotherapy in the rat brainstem with multiple catheters: a feasibility study. Childs Nerv Syst 25: 21-28
[128] Degen JW, Walbridge S, Vortmeyer AO, Oldfield EH, Lonser RR (2003) Safety and efficacy of convection-enhanced delivery of gemcitabine or carboplatin in a malignant glioma model in rats. J Neurosurg 99: 893-898

Eidesstattliche Versicherung

„Ich, Young Sill Kang, versichere an Eides statt durch meine eigenhändige Unterschrift, dass ich die vorgelegte Dissertation mit dem Thema: „Antitumor effect of PEG-ZnPP in Rat Glioma Cells, F98 and C6, and in Rat Brainstem Tumor Models“ selbstständig und ohne nicht offengelegte Hilfe Dritter verfasst und keine anderen als die angegebenen Quellen und Hilfsmittel genutzt habe.
Alle Stellen, die wörtlich oder dem Sinne nach auf Publikationen oder Vorträgen anderer Autoren beruhen, sind als solche in korrekter Zitierung kenntlich gemacht. Die Abschnitte zu Methodik (insbesondere praktische Arbeiten, Laborbestimmungen, statistische Aufarbeitung) und Resultaten (insbesondere Abbildungen, Graphiken und Tabellen werden von mir verantwortet.

Meine Anteile an etwaigen Publikationen zu dieser Dissertation entsprechen denen, die in der untenstehenden gemeinsamen Erklärung mit dem/der Betreuer/in, angegeben sind. Für sämtliche im Rahmen der Dissertation entstandenen Publikationen wurden die Richtlinien des ICMJE (International Committee of Medical Journal Editors; www.icmje.og) zur Autorenschaft eingehalten. Ich erkläre ferner, dass mir die Satzung der Charité – Universitätsmedizin Berlin zur Sicherung Guter Wissenschaftlicher Praxis bekannt ist und ich mich zur Einhaltung dieser Satzung verpflichte.

Die Bedeutung dieser eidesstattlichen Versicherung und die strafrechtlichen Folgen einer unwahren eidesstattlichen Versicherung (§156,161 des Strafgesetzbuches) sind mir bekannt und bewusst.“

Datum Unterschrift

Lebenslauf

Mein Lebenslauf wird aus datenschutzrechtlichen Gründen in der elektronischen Version meiner Arbeit nicht veröffentlicht.

Publikationsliste

05/2014 An Indolent Presentation of Gliomatosis Cerebri in an Elderly Patient: Posterior Fossa Decompression Prior to Treatment /Case Report : Cureus/ **Young Sill Kang**, Ami Raval, Karen S. Black, Jian Yi Li, Richard H. Blanck, Michael Schulder

03/2017 Altered Cerebrospinal Fluid Dynamics in Neurofibromatosis I ; Severe arachnoid thickening, which can also be caused by asymmetrical CSF pressure through sphenoid defect, may cause abnormal CSF dynamic in patients with neurofibromatosis type 1. / Child Nervous System/ **Young Sill Kang**, Eun-Kyung Park, Yong-Oock Kim, Ju-Seong Kim, Dong-Seok Kim, U. W. Thomale, Kyu-Won Shim

10/2017 Efficacy of Endoscopic Third Ventriculostomy in Patients with Normal Pressure Hydrocephalus / Journal of Geriatric Psychiatry and Neurology / **Young Sill Kang**, Eun-Kyung Park, Dong-Seok Kim, Ju-Seong Kim, U. W. Thomale, Kyu-Won Shim

Danksagung

Ich möchte mich hiermit bei Herrn Prof. Ulrich-Wilhelm Thomale, meinem Doktorvater, Leiter des selbständigen Arbeitsbereichs Pädiatrische Neurochirurgie der Charité Universitätsmedizin Berlin, bedanken, der mir die wunderbare Möglichkeit zur experimentellen Forschung gegeben hat, diese Arbeit vom Anfang bis zum Ende unter seiner Leitung durchzuführen. Auch für die ständige Betreuung mit Geduld und Verständnis möchte ich mich herzlich bedanken. Durch Zusammenarbeit seit Anfang meines Medizinstudiums hat er die Begeisterung für pädiatrische Neurochirurgie in mir geweckt.

Bei Herrn Prof. Dr. Jallo, Leiter der pädiatrischen Neurochirurgie in Johns Hopkins All Children’s Hospital, danke ich für die Möglichkeit, in seinem Arbeitskreis mein Experiment durchführen zu dürfen. Frau Prof. Tyler danke ich für die ständige Diskussions- sowie Hilfsbereitsschaft.

Ich bedanke mich bei meinen Geschwistern für liebevolles Antreiben und Unterstützung. Ganz besonders danke ich meinen Eltern, die mich mit ihrem Leben dazu motiviert haben, eine Ärztin zu werden.